Convection in a volcanic conduit recorded by bubbles

Rebecca J. Carey[1]*, Michael Manga[2], Wim Degruyter[2], Helge Gonnermann[3], Donald Swanson[4], Bruce Houghton[5], Tim Orr[4], and Matthew Patrick[4]

[1]ARC Centre of Excellence in Ore Deposits, and School of Earth Science, University of Tasmania, Sandy Bay, 7005 Tasmania, Australia
[2]Earth and Planetary Science, University of California–Berkeley, McCone Hall, Berkeley, California 94705, USA
[3]Department of Earth Science, Rice University, Houston, Texas 77005, USA
[4]Hawaiian Volcano Observatory, U.S. Geological Survey, Hawai'i Volcanoes National Park, Hawaii 96718, USA
[5]Geology and Geophysics Department, University of Hawai'i at Manoa, Honolulu, Hawaii 96822, USA

ABSTRACT

Microtextures of juvenile pyroclasts from Kīlauea's (Hawai'i) early A.D. 2008 explosive activity record the velocity and depth of convection within the basaltic magma-filled conduit. We use X-ray microtomography (μXRT) to document the spatial distribution of bubbles. We find small bubbles (radii from 5 μm to 70 μm) in a halo surrounding larger millimeter-size bubbles. This suggests that dissolved water was enriched around the larger bubbles—the opposite of what is expected if bubbles grow as water diffuses into the bubble. Such volatile enrichment implies that the volatiles within the large bubbles were redissolving into the melt as they descended into the conduit by the downward motion of convecting magma within the lava lake. The thickness of the small bubble halo is ~100–150 μm, consistent with water diffusing into the melt on time scales on the order of 10^3 s. Eruptions, triggered by rockfall, rapidly exposed this magma to lower pressures, and the haloes of melt with re-dissolved water became sufficiently supersaturated to cause nucleation of the population of smaller bubbles. The required supersaturation pressures are consistent with a depth of a few hundred meters and convection velocities of the order of 0.1 m s^{-1}, similar to the circulation velocity observed on the surface of the Halema'uma'u lava lake.

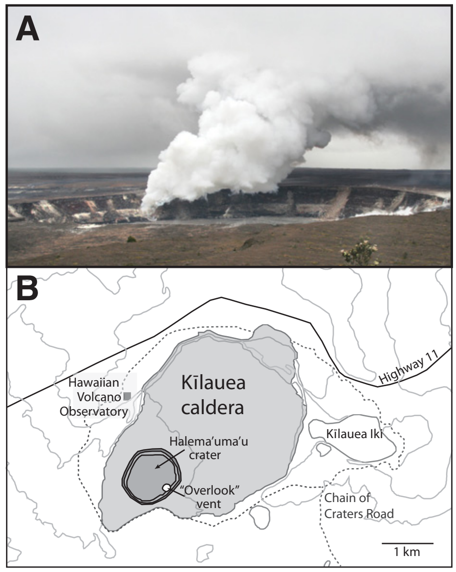

Figure 1. A: Photograph of the Overlook vent within Halema'uma'u crater at Kīlauea Volcano, Hawai'i. Vent diameter at this time was 39 m. Photo taken from the Hawaiian Volcano Observatory, view looking southeast, on 10 April 2008 by C. Heliker (U.S. Geological Survey). B: Map of Kīlauea's summit region, illustrating location of Halema'uma'u vent. At time of writing, vent diameter was 160 m (Orr et al., 2012).

INTRODUCTION

Lava-filled conduits are complex systems where degassing, cooling, and crystallization of magmas may generate convection. Measured magmatic gases, thermal imagery of heat flux, as well as the surface expression of convection on lava lakes and filled conduits all confirm that conduit convection occurs (e.g., Witter et al., 2004; Harris et al., 2005; Palma et al., 2008, 2011; Oppenheimer and Yirgu, 2002).

Since A.D. 2008, an active lava lake has been hosted within the "Overlook" vent, located in Halema'uma'u crater, which in turn is located within the summit caldera of Kīlauea Volcano, Hawai'i (Fig. 1). Rockfalls of the conduit and vent walls into this lava lake have triggered heightened degassing, ash production, and at times, explosive eruptions (Orr et al., 2013). The eruptions at Halema'uma'u provide a unique opportunity to study an active lava lake as the erupted pyroclasts sample magma from a range of depths. Volatile solubility in magmas is primarily pressure dependent and at depths of a few hundred meters or less; the predominant volatile species dissolved in the melt is water (Dixon et al., 1995; Newman and Lowenstern, 2002; Papale et al., 2006). Because bubbles nucleate and grow in response to decreasing pressure as magma rises toward the surface, we use the microtextures of the 9 April 2008 pyroclasts along with a model for water diffusion and bubble nucleation to estimate the depths and rates of magma convection in the shallow Halema'uma'u conduit.

*E-mail: rebecca.carey@utas.edu.au.

EXPLOSIVE ERUPTIONS OF THE OVERLOOK VENT

Although lava within the vent was not visible until 5 September 2008, volatile fluxes in great excess of background levels and semicontinuous eruption of juvenile ash and lapilli indicate that magma was degassing at shallow levels. The first appearance of juvenile tephra was on 23 March 2008, and eruptive activity continues to the present (September 2012). Throughout this time, several hundred shallow conduit-wall and vent collapses (Orr et al., 2013) have triggered explosive eruptions that produced lapilli with high number densities of small bubbles (Carey et al., 2012). Disruption of the lava-lake surface by rockfalls caused short-lived but rapid magma decompression, which we infer resulted in the nucleation of high numbers of small bubbles (Carey et al., 2012).

9 APRIL 2008 EXPLOSIVE ERUPTION AND EJECTA

On 9 April, an area of ~200 m^2 collapsed into the vent and triggered a small explosive eruption that lasted ~14.5 s (Fee et al., 2010). The pyroclastic deposit geometry and isomass data imply that ~1.3×10^5 kg of magma and wall-rock lithic clasts were erupted. Following the eruption, 100 juvenile pyroclasts were collected for analysis. From macroscopic clast observations and clast density, nine representative clasts were selected for thin-sectioning, synchrotron Fourier transform infrared spectroscopy (FTIR) analysis, and X-ray microtomography (μXRT) at the Advanced Light Source, Lawrence Berkeley National Laboratory (California, United States). The April ejecta was macroscopically and microtexturally heterogeneous (Fig. 2). Three textural types were observed: (1) fluidal, fluted dense clasts containing spheroidal bubbles 1–4 mm in diameter; (2) dense spinose clasts with a bubble-poor (<10 vol%) outer margin up to 1 cm thick, and a more coarsely vesicular interior composed of predominantly millimeter-diameter bubbles with spheroidal shapes; and (3) highly vesicular and microvesicular, golden-colored clasts with complexly shaped bubbles up to 4 mm across. One representative clast from each type was selected for μXRT.

All clasts show an unusual texture; large millimeter-sized bubbles that are surrounded by up to 150-μm-thick haloes containing high numbers of small isolated round bubbles of between 5 μm and 70 μm in diameter (Fig. 3). This texture is the focus of our study; however, clast type 2 has a higher density, which permits measurement of haloes (and vesicles contained

GEOLOGY, April 2013; v. 41; no. 4; p. 395–398; Data Repository item 2013109 | doi:10.1130/G33685.1

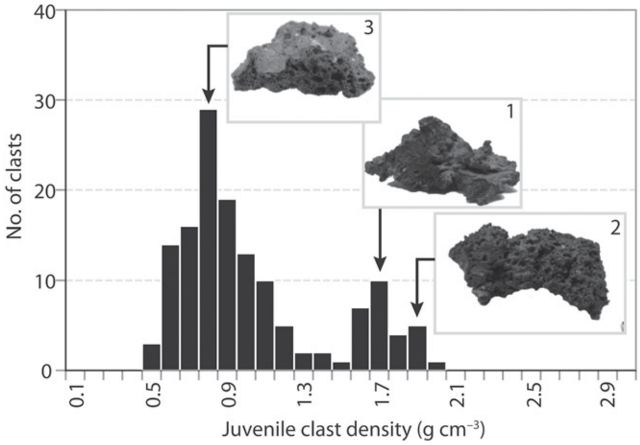

Figure 2. Juvenile clast density of the 9 April 2008 eruption sample. Superimposed on the plot are three representative clasts and their corresponding densities. Haloes of small bubbles around larger bubbles are most commonly observed in texture 2; however, they can be observed in other textures. We estimate that ~10%–15% of erupted clasts contain this microtexture.

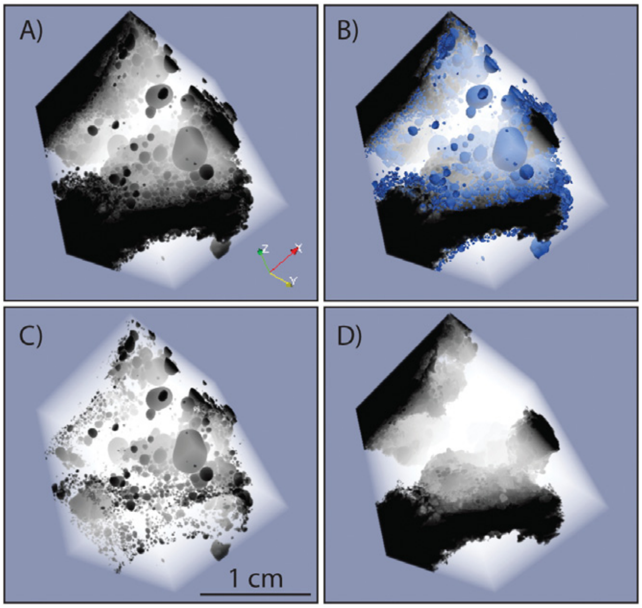

Figure 3. X-ray microtomographic renderings of segmented images from a texturally representative type 2 clast erupted on 9 April 2008. Haloes surround large millimeter-sized bubbles and are filled with 5–70-µm-sized bubbles and range up to 100 µm in thickness. A: Three-dimensional rendering of the segmented volume, where bubbles are black and glass is translucent white. B: Small bubble population. Bubbles with a diameter of 180 µm or less are blue within this volume. Small bubbles concentrate within the halo surrounding larger millimeter-sized bubbles. C: Spatial distribution of small bubbles within the volume. D: The large bubbles within this volume. The largest bubbles exceed size of the imaged volume; however they are macroscopically observed in the pyroclasts. Some small bubbles are connected to the largest neighboring bubble, which might either come from partial coalescence or a spatial resolution that was not high enough to capture the thin bubble wall. In all images, length of shortest side is 0.9 mm. X-Y-Z orientation of imaged volume is shown by colored axes in corner of A. At energies of 20 keV, radiographs with 200 ms exposure time were taken with 1400 rotation steps between angles of 0° and 180°. Images were cropped in order to capture inside of volume. Image segmentation was conducted using 3dma-rock (Lindquist and Venkatarangan, 1999) as applied to volcanic particles in Degruyter et al. (2010). Image visualization was conducted with open-source software ParaView (http://www.paraview.org).

within) with greater accuracy. Synchrotron FTIR analyses of the glass, including the small bubble haloes, showed uniform water concentrations of <0.1 wt% with no volatile gradients. This likely reflects the initial low water concentrations of the magma, the high diffusion rates of water in basaltic magmas, and the detection limits of the FTIR instrument.

The high number densities of small bubbles within the haloes reflect high nucleation rates and little time for bubble coalescence after nucleation (Carey et al., 2012). Furthermore, this unusual texture suggests that water concentrations were high enough only within the haloes to produce high rates of bubble nucleation. Watkins et al. (2012) identified a similar halo of small bubbles around large bubbles in rhyolite obsidian, where water concentration profiles show an enrichment of water adjacent to the large bubbles, equivalent to a pressure increase of ~10 MPa prior to eruption. As proposed by Watkins et al. (2012), this observation implies that the water within the large bubbles was resorbing back into the melt prior to eruption.

CONDUIT CONVECTION MODEL

The textures observed in Figure 3 can be used to constrain conduit dynamics. Specifically, the thickness of the haloes of small bubbles defines a diffusion length associated with bubble resorption during convection, whereas bubble number densities can provide estimates for water supersaturation, and thus, depth. Consequently, we consider a convecting lava lake with volatiles (water) exsolving during magma ascent, and then dissolving back into the melt around bubbles as the magma circulates back down the conduit. This process was interrupted when rockfalls impacted the lava, causing rapid decompression (Carey et al., 2012) and bubble nucleation in the water-enriched haloes.

Resaturation of Melt

Time variations in pressure (P) during convective cycling can be approximated as

$$P(t) = P_o + \Delta P_c \sin(2\pi t/\tau), \qquad (1)$$

where t is time, P_o and ΔP_c are the mean and change in pressure, and τ is the period of one convective overturn (circulation). Water diffusion in and out of the melt around individual bubbles creates a concentration boundary layer, the halo, over which water concentration changes by a factor of e with thickness (δ), where $\delta \propto \sqrt{D\tau}$ and D is the diffusivity of water. The diffusion of water in and out of bubbles is affected, however, by their expansion and contraction as they move up and down within the conduit, stretching and thickening the boundary layer, respectively. Existing analytical solutions (e.g., Fyrillas and Szeri, 1994) do not account for the nonlinearity of water solubility in basaltic melts nor the nonlinear change in radius with respect to pressure. We thus solve numerically for the thickness of the boundary layer upon bubble resorption for different bubble sizes, mean pressures (P_o), changes in pressure (ΔP_c), and periods of circulation (τ). The diffusivity depends on pressure and water content (Zhang et al., 2007), and water solubility is based on the model of Dixon (1997). We use an algorithm for bubble growth and volatile diffusion based on the formulation of Prousevitch et al. (1993) and viscosity based on the formulations of Hui and Zhang (2007) and Lensky et al. (2001). Steady-state boundary-layer thicknesses are reached after a few cycles of circulation, and we find that all cases are well described by

$$\delta = \sqrt{D\tau / 5}, \qquad (2)$$

(see Fig. DR1 in the GSA Data Repository[1]).

[1]GSA Data Repository item 2013109, Figure DR1 (scaling analysis) and Figure DR2 (nucleation rate as a function of supersaturation pressure), is available online at www.geosociety.org/pubs/ft2013.htm, or on request from editing@geosociety.org or Documents Secretary, GSA, P.O. Box 9140, Boulder, CO 80301, USA.

Microtextural analyses of three-dimensional (3-D) tomographic images indicate that melt shells with relatively high bubble number densities typically extend to δ ~100–150 µm around larger bubbles. Decompression during eruption will have thinned the boundary as the large bubble expanded. Neglecting diffusion during the eruption and assuming the magma is not permeable, so that all the gas remains in the large bubble, expansion from a pressure of 3 MPa (equivalent to a depth of 150 m for a density of 2000 kg m^{-3}; see below) to 0.1 MPa would thin δ by a factor of up to 10. In addition, the nucleation growth of small bubbles in the halo thickens the boundary layer by a factor of ~2. Thus, at depth δ may have been up to ~5 times thicker, or between 100 and 500 µm. Using $D = 1.3 \times 10^{-10}$ m^2 s^{-1} for basaltic magma at 1165 °C (Zhang et al., 2007), the calculated time scale τ for this length scale of diffusion is ~0.4×10^3 s to 1×10^4 s. Owing to the high permeability of vesicular basaltic magma (Saar and Manga, 1999), we suggest that there may have been little expansion of the large bubbles post-fragmentation, in which case τ would be near the lower end of this range.

Nucleation During Eruption

The unusual texture with small bubbles surrounding large ones has three requirements: (1) a mechanism to produce a water-enriched region around bubbles (here attributed to an increase in pressure due to downward convection); (2) the mean pressure P_o prior to eruption must be small enough that there is insufficient supersaturation for bubble nucleation outside of the haloes; and (3) ΔP_c must be large enough to create sufficient supersaturation for bubble nucleation within the haloes. For the clasts that erupt from well below that surface of the lava pond, we assume that the pressure fluctuations from the rockfall are damped.

Whether dissolved volatiles will nucleate new bubbles or diffuse into preexisting bubbles during eruption depends on the time scale for diffusion, τ_{diff}, compared with the time scale over which pressure decreases, τ_p. Given that the eruption time scale is much shorter (seconds) than the convection time scale τ (which is obtained from the diffusion time scale), the melt should remain supersaturated during the eruption, both in the boundary layer δ, and in the region farther from the large bubbles. However, the observation of high bubble densities in the haloes around large bubbles suggests that on eruptive time scales the supersaturation is great enough to nucleate bubbles within the haloes but not the rest of the melt. This provides a constraint on ΔP_c and P_o, which can be used to estimate depths to which the magma circulated.

We adopt a model for homogeneous nucleation based on classical nucleation theory (e.g., Mangan and Sisson, 2000):

$$J = \frac{2 n_o^2 V_m D \left(\frac{\phi\gamma}{kT}\right)^{\frac{1}{2}}}{a_o} \exp\left[-\frac{16\pi\gamma^3}{3kT\Delta P^2}\phi\right]$$

$$= J_o \exp\left[-\frac{16\pi\gamma^3}{3kT\Delta P^2}\phi\right], \qquad (3)$$

where Jo and J are the nucleation rate, n_o is the number density of dissolved water molecules, V_m is the volume of water molecules, k is the Boltzmann constant, T is temperature, a_o is the mean distance between water molecules, γ is the surface tension, and ΔP is the supersaturation pressure. ϕ is a factor that accounts for the decrease in surface energy for heterogeneous nucleation; its value is not known for basalt, so we use the product $\gamma\phi^{1/3} = 0.0091$ N/m measured by Hurwitz and Navon (1994) for rhyolite (equivalent properties are not available for basalt). Diffusivity is calculated from Zhang et al. (2007). We emphasize the considerable uncertainty in the parameters in Equation 3, and note that this nucleation model has not been tested for basalt.

The nucleation rate (number of bubbles per cubic meter per second) has an exponential dependence on supersaturation and will increase very rapidly beyond some threshold pressure, ~3 MPa for the adopted model parameters (Fig. DR2). We thus require that the mean circulation depth corresponds to pressures less than $P_o = 3$ MPa. For a bulk density $\rho_m = 1 - 2 \times 10^3$ kg m^{-3}, this pressure implies depths of convection $d = P_o/\rho_m g$ of ~150–300 m. Using our inferred diffusion time scale, we obtain convective velocities of $d/\tau \approx 0.02$–0.8 m s^{-1}, where the upper range corresponds to the case with limited post-fragmentation expansion of bubbles.

TIME AND LENGTH SCALES OF MAGMA CONVECTION

A combination of internal and external factors unique to Kīlauea's volcanic system provides a rare window into degassing and convection processes in a basaltic lava-filled conduit. In a convective cycle (Fig. 4), pressure cycling drives volatiles either to exsolve from or to resorb back into the melt (Fig. 4B). Bubble nucleation within the melt around milimeter-sized bubbles records magma circulation and pressure cycling. Using models for water diffusion and bubble nucleation in basaltic magma and the measured length scale of the bubble haloes, we estimate the depth to which magma is recycled in the shallow conduit (100–300 m), the time scales of convection (0.4×10^3 s to 1×10^4 s), and the convective velocities (0.02–0.8 m s^{-1}). The latter prediction is testable, and the range of our calculated vertical convective velocity is similar to that observed on the surface of the Halemaʻumaʻu lava lake (0.1–0.3 m s^{-1}).

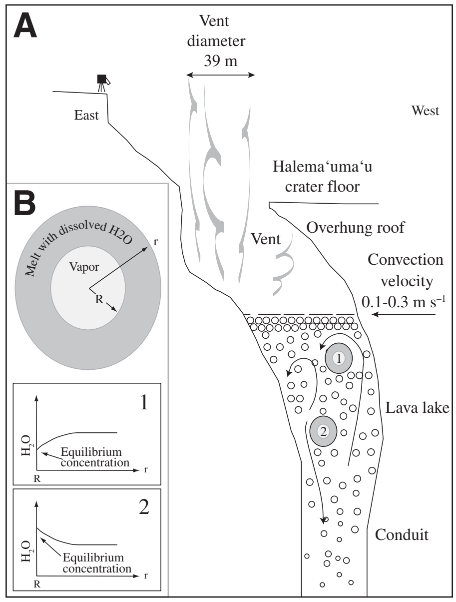

Figure 4. A: Schematic profile of Halemaʻumaʻu shallow conduit (Hawaiʻi), cavity, and vent system as it appeared in September 2008 when lava lake surface was first visible. During this time, the roof of the cavity was severely overhung and has proceeded to break throughout the course of the eruption, falling into the vent and triggering excess tephra to be erupted and, occasionally, short-duration explosive events (Patrick et al., 2011; Orr et al., 2013). B: Schematic diagram of packet of magma where each bubble is surrounded by layer of melt of thickness R-r, using spherical bubble approximation relevant to Halemaʻumaʻu basaltic lava lake system. In a convecting cycle, at depth, decreasing pressure (1) drives exsolution of volatiles and molar volume of gas to increase. Volatiles in the melt diffuse down a concentration gradient toward the melt-vapor interface where they exsolve. At depth, increasing pressure (2) causes the molar volume of gas to reduce, resulting in volatiles diffusing back into melt shell to a distance proportional to pressure. Strong pressure gradients in the system drive short-lived supersaturation and renewed nucleation of bubbles in zones that have relatively high volatiles, which in this system at depth is within the melt halo surrounding the preexisting larger bubbles.

GAS-MELT COUPLING IN CONVECTING CONDUITS

The microtextural observations described in this paper confirm that bubbles can be carried by the convecting magma to depths in excess of 100 m. We can calculate the critical size for bubbles to decouple from the magma, which occurs when their ascent speed owing to buoyancy is greater than the downward velocity of the convecting magma. The Stokes velocity of a bubble is

$$U_s = \frac{1}{3}\frac{\Delta\rho}{\mu} g R^2, \qquad (4)$$

where $\Delta\rho$ is the density difference between the melt and gas, μ is the fluid viscosity, g is gravitational acceleration, and R is bubble radius. The ratio of U_s to the speed of convection U_c is called the Stokes number and it determines the degree of coupling between the bubble and the melt. A bubble with Stokes number greater than ~1 indicates that the bubble largely ignores the fluid flow, whereas a bubble with Stokes number smaller than ~1 is coupled to the flow and is carried as a tracer. Choosing Stokes number U_s/U_c = 1 to separate coupled and decoupled flow, we have $U_s/U_c = 1$ from which we obtain an expression for critical bubble radius R_c:

$$R_c = \sqrt{3\frac{U_c}{g}\frac{\mu}{\Delta\rho}}. \quad (5)$$

Using convective velocities observed on the surface of the Halema'uma'u lava lake, a bubble needs a diameter >~10 cm to decouple from the magma and readily reach the surface. Vigorously convecting lava lakes like Halema'uma'u will lose their gas less efficiently than those that are convecting more slowly, as only the very large bubbles can escape from the flow. They therefore maintain enough potential energy in the form of exsolved water to react explosively to rockfalls. The bubbles preserved in the erupted clasts thus preserve a record of circulation depth, convection velocity, and the separation of bubbles from the melt in the conduit.

CONCLUSIONS

The minimum depth to which the Halema'uma'u lava lake overturns convectively can be estimated from pyroclast microtextures. As bubbles are advected downward by the convecting magma, water diffusively resorbs, creating boundary layers (haloes) with high water concentration. Short-lived and rapid decompression of the convecting magma, triggered by rockfalls into the lava lake, results in water supersaturation and high rates of bubble nucleation within these haloes. The width of the haloes constrains the characteristic diffusion time scale, whereas the bubble number density (assuming classical nucleation theory) constrains water concentrations, and hence, depth. The combination of depth and diffusion time yield convective velocities, compatible with measured surface velocities of the Halema'uma'u lava lake. The analyzed textures thus provide a rare but intriguing insight into the upper parts of the highly vigorous magmatic plumbing system of the most active volcano on Earth, where outgassing is likely never complete.

ACKNOWLEDGMENTS

This research was supported by National Science Foundation grants EAR-1049662, EAR-0810332, and EAR-1145187, and U.S. Geological Survey grant SV-ARRA-0004. We would like to thank Jocelyn McPhie, Dork Sahagian, Ed Llewelyn, Roger Denlinger, and two anonymous reviewers for editing a previous version of the manuscript. The FTIR and XRT analyses were conducted at the Advanced Light Source (ALS) at the Lawrence Berkeley National Laboratory in Berkeley, California, USA. We wish to thank the 8.3.2 and 1.4.3 ALS Beamline scientists Alastair McDowell, Dula Parkinson, Michael Martin, and Hans Bectel for all their helpful advice and technical assistance.

REFERENCES CITED

Carey, R., Manga, M., Degruyter, W., Swanson, D.A., Houghton, B.F., Orr, T., and Patrick, M., 2012, Externally triggered renewed bubble nucleation in basaltic magma: The October 12 2008 eruption at Halema'uma'u Overlook vent, Kilauea, Hawai'i, USA: Journal of Geophysical Research, doi:10.1029/2012JB009496 (in press).

Degruyter, W., Bachmann, O., and Burgisser, A., 2010, controls on the permeability in the volcanic conduit during the climactic phase of the Kos Plateau Tuff eruption (Aegean Arc): Bulletin of Volcanology, v. 72, p. 63–74, doi:10.1007/s00445-009-0302-x.

Dixon, J.E., 1997, Degassing of alkalic basalts: The American Mineralogist, v. 82, p. 368–378.

Dixon, J.E., Stolper, E.M., and Holloway, J.R., 1995, An experimental study of water and carbon dioxide solubilities in mid-ocean ridge basaltic liquids, part I: Calibration and solubility models: Journal of Petrology, v. 36, p. 1607–1631.

Fee, D., Garces, M., Patrick, M., Chouet, B., Dawson, P., and Swanson, D., 2010, Infrasonic tremor and degassing bursts from Halema'uma'u Crater, Kīlauea Volcano, Hawaii: Journal of Geophysical Research, v. 115, B11316, doi:10.1029/2010JB007642.

Fyrillas, M.M., and Szeri, A.J., 1994, Dissolution or growth of soluble spherical oscillating bubbles: Journal of Fluid Mechanics, v. 277, p. 381–407, doi:10.1017/S0022112094002806.

Harris, A.J.L., Carniel, R., and Jones, J., 2005, Identification of variable convective regimes at Erta Ale Lava Lake: Journal of Volcanology and Geothermal Research, v. 142, p. 207–223, doi:10.1016/j.jvolgeores.2004.11.011.

Hui, H., and Zhang, Y., 2007, Toward a general viscosity equation for natural anhydrous and hydrous melts: Geochimica et Cosmochimica Acta, v. 71, p. 403–416, doi:10.1016/j.gca.2006.09.003.

Hurwitz, S., and Navon, O., 1994, Bubble nucleation in rhyolitic melts: Experiments at high pressure, temperature, and water content: Earth and Planetary Science Letters, v. 122, p. 267–280, doi:10.1016/0012-821X(94)90001-9.

Lensky, N.G., Lyakhovsky, V., and Navon, O., 2001, Radial variations of melt viscosity around growing bubbles and gas overpressure in vesiculating magmas: Earth and Planetary Science Letters, v. 186, p. 1–6, doi:10.1016/S0012-821X(01)00227-8.

Lindquist, W.B., and Venkatarangan, A., 1999, Investigating 3D geometry of porous media from high resolution images: Physics and Chemistry of the Earth, v. 24, p. 593–599.

Mangan, M.T., and Sisson, T.W., 2000, Delayed, disequilibrium degassing in rhyolite magma: Decompression experiments and implications for explosive volcanism: Earth and Planetary Science Letters, v. 183, p. 441–455, doi:10.1016/S0012-821X(00)00299-5.

Newman, S., and Lowenstern, J., 2002, VolatileCalc: A silicate melt-H_2O-CO_2 solution model written in Visual Basic for Excel: Computers & Geosciences, v. 28, p. 597–604, doi:10.1016/S0098-3004(01)00081-4.

Oppenheimer, C., and Yirgu, G., 2002, Thermal imaging of an active lava lake: Erta 'Ale volcano, Ethiopia: International Journal of Remote Sensing, v. 23, p. 4777–4782, doi:10.1080/01431160110114637.

Orr, T.R., Patrick, M.R., Swanson, D.A., Weston, A., Thelen, A., and Wilson, D.C, 2013, Explosive eruptions triggered by rockfalls at Kīlauea Volcano, Hawai'i: Geology, v. 41, doi:10.1130/G33564.1 (in press).

Palma, J.L., Blake, S., and Calder, E.S., 2011, Constraints on the rates of degassing and convection in basaltic open-vent volcanoes: Geochemistry Geophysics Geosystems, v. 12, Q11006, doi:10.1029/2011GC003715.

Papale, P., Moretti, R., and Barbato, D., 2006, The compositional dependence of the saturation surface of $H_2O + CO_2$ fluids in silicate melts: Chemical Geology, v. 229, p. 78–95, doi:10.1016/j.chemgeo.2006.01.013.

Patrick, M.R., Wilson, D., Fee, D., Orr, T., and Swanson, D., 2011, Shallow degassing events as a trigger for very-long-period seismicity at Kīlauea Volcano, Hawai'i: Bulletin of Volcanology, v. 73, p. 1179–1186, doi:10.1007/s00445-011-0475-y.

Prousevitch, A.A., Sahagian, D.L., and Anderson, A.T., 1993, Dynamics of diffusive bubble growth in magmas: Isothermal case: Journal of Geophysical Research, v. 98, p. 22,283–22,307, doi:10.1029/93JB02027.

Saar, M.O., and Manga, M., 1999, Permeability of vesicular basalts: Geophysical Research Letters, v. 26, p. 111–114, doi:10.1029/1998GL900256.

Watkins, J.M., Manga, M., and DePaolo, D.J., 2012, Bubble geobarometry: A record of pressure changes, degassing and regassing and Mono Craters: California Geology, v. 40, p. 699–702.

Witter, J.B., Kress, V.C., Delmelle, P., and Stix, J., 2004, Volatile degassing, petrology, and magma dynamics of the Villarica Lava Lake, Southern Chile: Journal of Volcanology and Geothermal Research, v. 134, p. 303–337, doi:10.1016/j.jvolgeores.2004.03.002.

Zhang, Y., Xu, Z., Zhu, M., and Wang, H., 2007, Silicate melt properties and volcanic eruptions: Reviews of Geophysics, v. 45, RG4004, doi:10.1029/2006RG000216.

Manuscript received 29 May 2012
Revised manuscript received 3 October 2012
Manuscript accepted 11 October 2012

Printed in USA